Unraveling Molecular Complexity of Phosphorylated Human Cardiac Troponin I by Top Down Electron Capture Dissociation/Electron Transfer Dissociation Mass Spectrometry*[S]

Vlad Zabrouskov‡, Ying Ge§¶, Jae Schwartz‡, and Jeffery W. Walker§‖

Cardiac troponin I (cTnI), the inhibitory subunit of the thin filament troponin-tropomyosin regulatory complex, is required for heart muscle relaxation during the cardiac cycle. Expressed only in cardiac muscle, cTnI is widely used in the clinic as a serum biomarker of cardiac injury. *In vivo* function of cTnI is influenced by phosphorylation and proteolysis; therefore analysis of post-translational modifications of the intact protein should greatly facilitate the understanding of cardiac regulatory mechanisms and may improve cTnI as a disease biomarker. cTnI (24 kDa, pI ~ 9.5) contains twelve serine, eight threonine, and three tyrosine residues, which presents a challenge for unequivocal identification of phosphorylation sites and quantification of positional isomers. In this study, we used top down electron capture dissociation and electron transfer dissociation MS to unravel the molecular complexity of cTnI purified from human heart tissue. High resolution MS spectra of human cTnI revealed a high degree of heterogeneity, corresponding to phosphorylation, acetylation, oxidation, and C-terminal proteolysis. Thirty-six molecular ions of cTnI were detected in a single ESI/FTMS spectrum despite running as a single sharp band on SDS-PAGE. Electron capture dissociation of monophosphorylated cTnI localized two major basal phosphorylation sites: a well known site at Ser^{22} and a novel site at Ser^{76}/Thr^{77}, each with partial occupancy (Ser^{22}: 53%; Ser^{76}/Thr^{77}: 36%). Top down MS^3 analysis of diphosphorylated cTnI revealed occupancy of Ser^{23} only in diphosphorylated species consistent with sequential (or ordered) phosphorylation/dephosphorylation of the $Ser^{22/23}$ pair. Top down MS of cTnI provides unique opportunities for unraveling its molecular complexity and for quantification of phosphorylated positional isomers thus allowing establishment of the relevance of such modifications to physiological functions and disease status. *Molecular & Cellular Proteomics 7:1838–1849, 2008.*

Cardiac troponin I (cTnI)[1], the inhibitory subunit of the key thin filament troponin-tropomyosin regulatory complex, plays a critical role in Ca^{2+}-mediated regulation of cardiac muscle contraction and relaxation (1–7). cTnI is one of three troponin I genes found in all vertebrates but is expressed only in the heart. It has become a biomarker of choice for detecting cardiac muscle injury because of its absence from skeletal muscle (8). Altered phosphorylation of cTnI and other key myofilament proteins can have dramatic effects on cardiac function (9–11). Hyperphosphorylation of cTnI has been proposed to contribute causally to cardiac dysfunction in the transition from compensated hypertrophy to heart failure (10). Phosphorylation of cTnI has been extensively studied (5–7, 10–14) and known to be regulated by cAMP-dependent protein kinase (PKA), protein kinase C (PKC), p21-activated kinase, cyclic GMP-dependent protein kinase, and protein kinase D. At least five serine/threonine phosphorylation sites of cTnI have been identified, including $Ser^{23/24}$ ($Ser^{22/23}$ excluding the initiating methionine), $Ser^{43/45}$, and Thr^{144}, based on *in vitro* phosphorylation studies (3–7, 10–14). However, to our knowledge, the *in vivo* basal phosphorylation sites of cTnI purified directly from heart tissues have not yet been characterized. cTnI (24 kDa, pI ~ 9.5) has twelve serine, eight threonine, and three tyrosine residues, which presents a major challenge for unequivocal determination of the specific phosphorylation sites as well as relative quantification of the resulting positional isomers.

A "top down" mass spectrometry (MS) approach has been shown to be uniquely suited for characterization of proteins (10–200 kDa) with complex post-translational modifications (15–30). In the traditional "bottom up" approach, proteins of interest are digested with an enzyme (*e.g.* trypsin) either in gel or in solution prior to MS and MS/MS analysis (31–33). This

From ‡Thermo Fisher Scientific, San Jose, California 95134 and the §Human Proteomics Program and Department of Physiology, School of Medicine and Public Health, University of Wisconsin, Madison, Wisconsin 53706

Received, October 31, 2007, and in revised form, March 24, 2008
Published, MCP Papers in Press, April 28, 2008, DOI 10.1074/mcp.M700524-MCP200

[1] The abbreviations used are: cTnI, cardiac troponin I; ECD, electron capture dissociation; ETD, electron transfer dissociation; CAD, collisionally activated dissociation; IRMPD, infrared multiphoton dissociation; LTQ, linear ion trap; PKA, cAMP-dependent protein kinase; PKC, protein kinase C; S/N, signal to noise ratio; AR, abundance ratio; PPO%, phosphorylation occupancy; MS, mass spectrometry; MS/MS, tandem mass spectrometry.

provides a fast, reliable identification of the protein as well as certain types of post-translational modification. However, bottom up analysis has intrinsic limitations for characterizing protein modifications because the peptide sequences recovered from the digestion typically represent only partial coverage of the protein sequence, and most of the tryptic peptides are relatively small resulting in a loss of correlation between modifications on disparate portions of the protein (34, 35). The top down strategy measures molecular weights of intact proteins and dissociates these intact molecular ions directly in the gas phase providing highly reliable detection and characterization of sequence alterations and post-translational modifications (15–30, 36). Use of the newly developed MS/MS techniques of electron capture dissociation (ECD) (37, 38) and electron transfer dissociation (ETD) (39) greatly improves both the efficiency and sequence coverage in top down analyses. ECD and ETD cleave NH–CHR bonds to produce mainly *c* and $z^{\bullet}$ ions, complementary to those from the well developed energetic dissociation methods such as collisionally activated dissociation (CAD) (40) and infrared multiphoton dissociation (IRMPD) (41) that cleave CO–NH bonds to produce *b* and *y* fragment ions. The most important feature of ECD and ETD is that they are nonergodic (37–39), which makes them extremely powerful in locating labile post-translational modifications in peptides or intact proteins (42–47).

The importance of quantification in proteomics is increasingly appreciated (48), and various technologies developed for quantitative proteomics including but not limited to isotope-coated affinity tags (ICAT) (49), amine-reactive isobaric tags (iTRAQ) (50), and stable isotope labeling by amino acids in cell culture (SILAC) (51, 52) have generated widespread interest. However, estimating the relative abundance of isomeric protein species with specific modifications remains a challenge in proteomics and yet is extremely important for elucidating biological function. A top down MS approach is especially attractive because the ionization efficiency of intact proteins is much less affected by the presence of modifying groups in comparison with peptides (25, 35). Recently a top down MS strategy with ECD has been successfully used for quantitative characterization of positional isomers with stable modifications and partial site occupancies (25, 27). MS analysis of protein phosphorylation still remains a difficult task in proteomics because of the substoichiometric phosphorylation and the facile loss of phosphoric acid (53, 54). Hence quantification of phosphorylated positional isomers is extremely challenging and to our knowledge has not yet been reported in the literature. In this study, we used top down ECD and ETD mass spectrometry for unraveling the molecular complexity of the clinically important human cTnI and quantification of the labile phosphorylated positional isomers.

EXPERIMENTAL PROCEDURES

Top Down Mass Spectrometry—Human cTnI was immunoaffinity-purified from human heart tissue (Calbiochem, San Diego, CA), dissolved in water/acetonitrile/formic acid (50:50:0.1) at 0.1 μg/μl, and loaded into an externally coated nanospray emitter with a 2-μm inner diameter (New Objective Inc., Woburn, MA) using a spray voltage of 1.0–1.4 kV *versus* the inlet of the mass spectrometer, resulting in a flow of 20–50 nl/min. Intact protein molecular ions were analyzed using a linear trap/FTICR (LTQ FT Ultra) hybrid mass spectrometer (Thermo Scientific Inc., Bremen, Germany). Ion transmission into the linear trap and further to the FTICR cell was automatically optimized for maximum ion signal. The target values (the approximate number of accumulated ions) for a full MS scan linear trap scan, FTICR cell (FT) scan, MS^n linear trap scan, and MS^n FTICR scan were 3×10^4, 10^6, 10^4, and 5×10^5, respectively. The resolving power of the FTICR mass analyzer was set at 100,000 $m/\Delta m_{50\%}$ at m/z 400, resulting in one scan/s acquisition rate. Individual charge states of the protein molecular ions were first isolated and then dissociated by ECD using 2% "electron energy" and a 45-ms duration time with no delay. Up to 3000 transients were averaged per spectrum to ensure high quality ECD spectra from low abundance precursor ions. Alternatively precursor ions were dissociated by IRMPD in the ICR cell. The laser duration and intensity were adjusted to result in 80–90% precursor depletion. All FTICR spectra were processed with Xtract software (FT programs 2.0.1.0.6.1.4, Xcalibur 2.0.5, Thermo Scientific Inc., Bremen, Germany) using a S/N threshold of 1.2 and fit factor of 10% and validated manually. The resulting monoisotopic mass lists were further searched using ProSightPC software (version 1.0, Thermo Scientific Inc., San Jose, CA) against a human database (UniProt, released December 6, 2005, containing 33,592 basic sequences) with monoisotopic precursor tolerance of 400 Da, 10-ppm monoisotopic fragment tolerance, and 10 minimum required matches. The static (mono-, di-, and tri-) methylations, phosphorylations, and acetylations were considered during the search. The top candidate intact protein sequence with a P-score better than 10^{-3} was then used to assign the previously unassigned fragments using a single protein search mode with 10-ppm monoisotopic precursor and fragment tolerance; variable phosphorylations of Ser, Thr, and Tyr residues; sequence truncations on both termini; and 10 minimum required matches. The M_r values reported in the study are all most abundant masses and the mass difference (in units of 1.00235 Da) between the most abundant isotopic peak, and the monoisotopic peak is denoted in italics after each M_r value.

ETD experiments were performed using LTQ ETD with a 100-ms reaction time and a 2×10^5 anion target for the ETD reagent fluoranthene produced by a negative chemical ionization source attached to the back of the linear trap. Up to 100 scans were averaged to achieve desirable S/N on MS^3 ETD fragments. The resulting MS^3 spectra were assigned manually to produce sequence tags that were used to pinpoint the location of phosphorylated residue(s) within the MS^2 fragment.

Bottom Up Mass Spectrometry with Limited Glu-C Digestion—Ten micrograms of the human cTnI were dissolved in 25 mM ammonium bicarbonate buffer, pH 7.8, and digested with 0.2 μg of endoproteinase Glu-C (also known as V8 protease) (Calbiochem, San Diego, CA) for 1 h at 37 °C, and the resulting peptide mixture (equivalent to 1 μg of protein) was separated by LC using a C_{18} 150-μm-inner diameter, 100-mm-long column (Microtech Scientific, Vista, CA) with a 200 nl/min flow rate and 45-min gradient. The peptide mixtures were analyzed using an LTQ Orbitrap XL mass spectrometer (Thermo Scientific Inc., Bremen, Germany). In these LC/MS experiments, a full MS scan in the Orbitrap was acquired in parallel with three data-dependent MS/MS scans in the LTQ. Dynamic Exclusion™ was used with a single repeat count and 7-min exclusion duration. High resolution full-scan spectra (60,000 $m/\Delta m_{50\%}$ at m/z 400) were acquired using a single microscan with 700-ms maximum ion injection time. For MS/MS, precursor ions were activated using 25% normalized

collision energy at the default activation q of 0.25 and detected in the linear ion trap. The LC/MS/MS data were searched with the Mascot search engine (version 2.2, Matrix Sciences Ltd., London, UK) against a human database (IPI_human HUMAN_v3_27, containing 67,528 sequences) with 5-ppm precursor mass accuracy, 0.8-Da fragment mass accuracy, ESI-FTICR instrument type, and a maximum of three missed cleavages for V8-E enzyme and allowing for fixed acetylation on the protein N terminus and variable phosphorylation on Ser, Thr, and Tyr residues. The results were filtered using a significance threshold of $p < 0.001$ and ion score of 15, and only "bold red" peptide matches were considered.

Calculation of Phosphorylation Occupancies of Multiple Sites—To quantitatively determine the partial phosphorylation occupancy of each site, ECD experiments were performed on the M^{33+}, M^{32+}, and M^{31+} charge states of the molecular ions of unphosphorylated (23,554.757-*14* at *m/z* 714.8, 737.1, and 760.8, respectively) and monophosphorylated isoform III (23,634.728-*14* at *m/z* 717.2, 739.6, and 763.4, respectively) with three replicates per charge state. The peak intensities of the resulting unphosphorylated *c* fragment ions (S/N > 3) were used to calculate the partial phosphorylation occupancy for each distinct phosphorylation site. The absolute abundance of the most abundant isotope of each individual unphosphorylated fragment was first normalized *intraspectrum versus* the fragments whose relative abundances had not changed after phosphorylation (analogous to "internal standard"). Such normalized abundances were then compared *interspectra* between unphosphorylated and phosphorylated precursors. The abundance ratio (AR) and phosphorylation occupancy (PPO%) were calculated according to Equations 1 and 2. The partial occupancy of individual phosphorylation sites was calculated as a relative percentage of their full occupancy.

$$AR = \frac{(Ax/Ai)^p}{(Ax/Ai)^u} \quad \text{(Eq. 1)}$$

and

$$PPO\% = [1 - AR] \times 100\% \quad \text{(Eq. 2)}$$

where Ax is the absolute abundance of the most abundant isotope of each individual unphosphorylated *c* fragment ion, Ai is the absolute abundance of the most abundant isotope of the "internal standard" *c* fragment ion, p represents the monophosphorylated form, and u represents the unphosphorylated form.

The S.E. was calculated for each fragment AR ($n = 18$ (three replicates of six internal standard *c* ions)). Analytical reproducibility was assessed using three replicates with the three most abundant charge states.

RESULTS

High Resolution Mass Spectrometry Analysis of Human cTnI—Human cTnI was immunoaffinity-purified from nominally healthy adult human heart tissue. Its size and relative purity were confirmed by SDS-PAGE and Coomassie Blue staining (Fig. 1*D*). The protein sample was analyzed by top down mass spectrometry with an LTQ FT Ultra. Direct electrospray ionization analysis produced a high resolution multiply charged mass spectrum as shown in Fig. 1*A*. The deconvoluted MS spectrum for cTnI is shown in Fig. 1*B*, revealing 36 molecular isoforms of the cTnI protein. The molecular weights, their tentative assignments based on accurate molecular mass, and the normalized relative abundances of the major and minor components are summarized in Table I. The

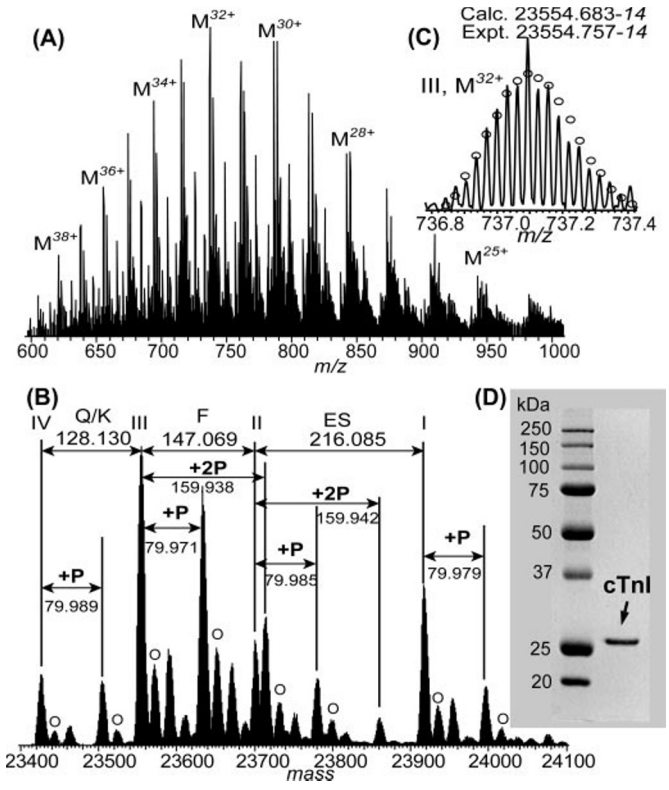

FIG. 1. **High resolution ESI/MS analysis of intact cTnI purified from human heart tissue.** *A*, full mass spectrum of multiply charged cTnI molecular ions. *B*, Xtract deconvoluted spectrum of multiply charged intact cTnI molecular ions as shown in *A*. *Roman numerals* indicate four different C-terminally truncated isoforms of cTnI. Each of the isoforms is also present as +80- and +160-Da forms (mono- and diphosphorylated (+*P* and +*2P*)). Oxidized species are indicated by "*O*." *C*, isotopically resolved molecular ion of isoform III (M^{32+}). *Circles* represent the theoretical abundance isotopic distribution of the isotopic peaks corresponding to the assigned mass. *D*, one-dimensional SDS-PAGE analysis of human cTnI stained with Coomassie Blue. *Calc.*, calculated; *Expt.*, experimental.

identities of the most abundant components of cTnI with masses of 23,554.757-*14* (isoform III; Fig. 1*C*), 23,634.728-*14*, and 23,714.695-*14* Da were confirmed by ECD and IRMPD experiments using an absolute mass search mode in ProSightPC. They corresponded to the N-terminal Ala-acetylated product of cTnI with the removal of Met from the N terminus and a loss of Phe-Glu-Ser residues from the C terminus (calculated M_r = 23,554.683-*14*) and its mono- and diphosphorylated isoforms, respectively. These positive identifications were supported by high P-scores of 8.6×10^{-29} and 3.6×10^{-10} for isoform III and its monophosphorylated form (from ECD spectra of 23,554.757-*14*- and 23,634.728-*14*-Da parent ions, 32+, at *m/z* 737 and 739.5, respectively) and a P-score of 4×10^{-4} for its diphosphorylated form (from IRMPD spectrum of 23,714.695-*14*-Da parent ion, 32+, at *m/z* 742). The other two forms with molecular weights of 23,701.826-*14* (isoform II) and 23,426.662-*14* (isoform IV) matched with N-terminal Ala-acetylated truncated products

TABLE I
Identification and relative quantification of major and minor components observed in ESI/FT MS spectrum of human cTnI

Observed M_r-*14*	Calculated M_r-*14*[a]	Error	Tentative identification[b]	Absolute abundance	Relative abundance
		ppm			%
23,426.662	23,426.588	3.1	IV	2,540	4.5
23,442.655	23,442.584	3.0	IV+O	227	0.4
23,461.627			No ID	262	0.5
23,506.651	23,506.554	4.0	IV+P	1,790	3.1
23,522.613	23,522.550	2.6	IV+P+O	258	0.5
23,538.629	23,538.546	3.5	IV+P+2O	272	0.5
23,554.757	23,554.683	3.1	III	8,520	14.9
23,570.748	23,570.679	2.9	III+O	1,520	2.7
23,586.716	23,586.675	1.7	III+2O and IV+2P	235	0.4
23,589.733			No ID	2,420	4.2
23,634.728	23,634.649	3.3	III+P	7,780	13.6
23,650.717	23,650.645	3.0	III+P+O	2,880	5.1
23,670.708			No ID	2,130	3.7
23,686.717			No ID	933	1.6
23,701.826	23,701.751	3.1	II	2,840	5.0
23,714.695	23,714.615	3.3	III+2P	3,880	6.8
23,730.684	23,730.611	3.0	III+2P+O	1,610	2.8
23,749.680			No ID	995	1.7
23,765.677			No ID	387	0.7
23,781.811	23,781.717	3.9	II+P	1,710	3.0
23,797.757	23,797.713	1.8	II+P+O	510	0.9
23,813.768	23,813.679	3.7	II+P+2O	228	0.4
23,829.657	23,829.645	0.5	II+P+3O	262	0.5
23,845.796	23,845.611	7.7	II+P+ 4O	140	0.2
23,861.768	23,861.683	3.5	II+2P	268	0.5
23,877.81	23,877.679	5.5	II+2P+O	155	0.3
23,917.911	23,917.826	3.5	I	4,540	8.0
23,933.887	23,933.822	2.7	I+O	250	0.4
23,952.865			No ID	1,730	3.0
23,968.859			No ID	281	0.5
23,984.793			No ID	738	1.3
23,997.890	23,997.792	4.1	I+P	1,670	2.9
24,013.859	24,013.788	3.0	I+P+O	988	1.7
24,029.847	24,029.784	2.6	I+P+2O	2,080	3.6
24,077.733	24,077.758	−1.0	I+2P	124	0.2
24,093.782	24,093.724	2.4	I+2P+O	341	0.6

[a] Calculated M_r is based on the amino acid sequence of entry name TNNI3_human obtained from the Swiss-Prot sequence database.
[b] Roman numerals indicate four different C-terminal truncated isoforms of N-terminally acetylated cTnI (I, residues 1–209; II, residues 1–207; III, residues 1–206; IV, residues 1–205). "P" stands for phosphorylation, and "O" stands for oxidation. Tentative identifications were not assigned ("No ID") for the cases where overlapping isotopic peaks were observed.

with Glu-Ser or Lys-Phe-Glu-Ser residues removed from the C terminus, respectively. The protein isoform with molecular weight of 23,917.911-*14* (isoform I) agrees with the molecular weight of the N-terminal Ala-acetylated full sequence of cTnI in the human database. No further MS/MS experiments were undertaken to confirm these assignments. Other major components of the sample matched with either mono- or diphosphorylated isoforms I–IV or oxidized products. Relative quantification of four truncated isoforms (I–IV) including modified and unmodified forms is summarized in Table II. The relative abundances of un-, mono-, and diphosphorylated forms observed for cTnI molecules are summarized in Table III. The amino acid sequences and molecular weights of the four human cTnI isoforms (I–IV) are shown in Table IV.

TABLE II
Relative quantification of four isoforms of human cTnI (I–IV) including modified and unmodified forms as assigned in Table I

cTnI isoform	Combined absolute abundance	Relative abundance
		%
I (Ac1–209)	9,993	21.0
II (Ac1–207)	6,113	12.8
III (Ac1–206)	26,425	55.5
IV (Ac1–205)	5,087	10.7
Sum	47,618	100

Localization of Basal Phosphorylation Sites in the Monophosphorylated cTnI Isoform III—Each of the cTnI isoforms (I–IV) existed in three states, M, M + 80, and M + 160,

representing un-, mono-, and diphosphorylated molecular species, respectively. To map basal phosphorylation sites, the individual charge state (M^{32+}) of the monophosphorylated isoform III was isolated and dissociated by ECD (Fig. 2). Masses derived from the resulting ECD spectra were assigned to fragments expected from the predicted sequence of cTnI with N-terminal Ala acetylation and C-terminal truncation of Phe-Glu-Ser residues (root mean square = 3.1 ppm). A single ECD experiment generated 37 *c* and 30 $z^{\bullet}$ fragment ions representing 65 cleavages of the total 205 NH–CH available backbone bonds in isoform III, confirming N-terminal Ala acetylation and the C-terminal truncation (Fig. 3 and supplemental Tables 1 and 2). The fact that only unphosphorylated *c* fragment ions were detected for c_9–c_{21} but a mixture of un- and monophosphorylated ions was observed for c_{22}–c_{113} fragments unambiguously assigned one phosphorylation site to Ser^{22}. Partial occupancy of this site was indicated by the co-existence of un- and monophosphorylated c_{22}–c_{113} ions. The presence of both unphosphorylated and monophosphorylated c_{66} ions in the ECD spectrum (Fig. 2, *inset*) indicates that some protein positional isomers have a phosphorylation site before (or on) residue 66 and that the rest are phosphorylated after residue 66. The observation of predominantly unphosphorylated $z^{\bullet}_{100}$ ions suggests that there are no major phosphorylation sites in isoform III after residue 106 (residues 206–100). Therefore, there must be a major phosphorylation site between residues 67 and 106; the only residues with side chain hydroxyls are Ser^{76} and Thr^{77}.

TABLE III
Relative quantification of overall un-, mono-, and diphosphorylated human cTnI including all four isoforms (I–IV) as assigned in Table I

cTnI phosphorylated form	Combined absolute abundance	Relative abundance
		%
Unphosphorylated	20,672	43.4
Monophosphorylated	20,568	43.2
Diphosphorylated	6,378	13.4
Sum	47,618	100

The monophosphorylation site at Ser^{22} was also verified with MS^3 ETD experiments (Fig. 4). First the individual charge state (M^{32+} at *m/z* 739.6) of monophosphorylated isoform III of cTnI (Fig. 4*A*) was dissociated in the ion trap using CAD (Fig. 4*E*). The dominant neutral loss of 80 Da was observed in the CAD spectrum (Fig. 4*C*) as phosphorylation is labile under the energetic dissociation conditions of CAD (or IRMPD). It is also possible that a fraction of the ions at *m/z* 683.545 could be unphosphorylated $b_{31}{}^{5+}$ fragments, MS/MS products of the monophosphorylated M^{32+} precursor ions. The abundant monophosphorylated b_{31} fragment (Fig. 4, *C* and *D*) (its identity was separately confirmed by high resolution accurate mass MS^2 IRMPD experiments; Fig. 4*B*) was further isolated and fragmented using ETD. The sequential doubly charged c_{13}–c_{25} fragment ions verified one phosphorylation at Ser^{22} (Fig. 4*F* and supplemental Table 3).

Determination of Phosphorylation Occupancies in Monophosphorylated cTnI—ECD experiments were performed individually on unphosphorylated and monophosphorylated cTnI isoform III to quantify phosphorylation occupancy of each site. Given that the first N-terminal phosphorylated res-

TABLE IV
The amino acid sequences and molecular weights of the four human cTnI isoforms

cTnI isoform	Amino acid sequence	Sequence modifications to TNNI3_human[a]	Calculated M_r-14[a]
I (Ac1–209)	ADGSSDAARERPAPAPIRRRSSNYRAYATEPHAKKKSKISASR KLQLKTLLLQIAKQELEREAEERRGEKGRALSTRCQPLELT GLGFAELQDLCRQLHARVDKVDEERYDIEAKVTKNITEIADL TQKIFDLRGKFKRPTLRRVRISADAMMQALLGARAKESLDLRA HLKQVKKEDTEKENREVGDWRKNIDALSGMEGRKKKFES	N-terminal acetylation	23,917.826
II (Ac1–207)	ADGSSDAARERPAPAPIRRRSSNYRAYATEPHAKKKSKISASR KLQLKTLLLQIAKQELEREAEERRGEKGRALSTRCQPLELTG LGFAELQDLCRQLHARVDKVDEERYDIEAKVTKNITEIAD LTQKIFDLRGKFKRPTLRRVRISADAMMQALLGARAKESLDLR AHLKQVKKEDTEKENREVGDWRKNIDALSGMEGRKKKF	N-terminal acetylation and C-terminal truncation of Glu-Ser	23,701.751
III (Ac1–206)	ADGSSDAARERPAPAPIRRRSSNYRAYATEPHAKKKSKISASRK LQLKTLLLQIAKQELEREAEERRGEKGRALSTRCQPLELTGLG FAELQDLCRQLHARVDKVDEERYDIEAKVTKNITEIADLTQK IFDLRGKFKRPTLRRVRISADAMMQALLGARAKESLDLRAHL KQVKKEDTEKENREVGDWRKNIDALSGMEGRKKK	N-terminal acetylation and C-terminal truncation of Phe-Glu-Ser	23,554.683
IV (Ac1–205)	ADGSSDAARERPAPAPIRRRSSNYRAYATEPHA KKKSKISASRKLQLKTLLLQIAKQELEREAEERRG EKGRALSTRCQPLELTGLGFAELQDLCRQLHARVDKVDEER YDIEAKVTKNITEIADLTQKIFDLRGKFKRPTLRRVR ISADAMMQALLGARAKESLDLRAHLKQVKKEDTEK ENREVGDWRKNIDALSGMEGRKK	N-terminal acetylation and C-terminal truncation of Lys-Phe-Glu-Ser	23,426.588

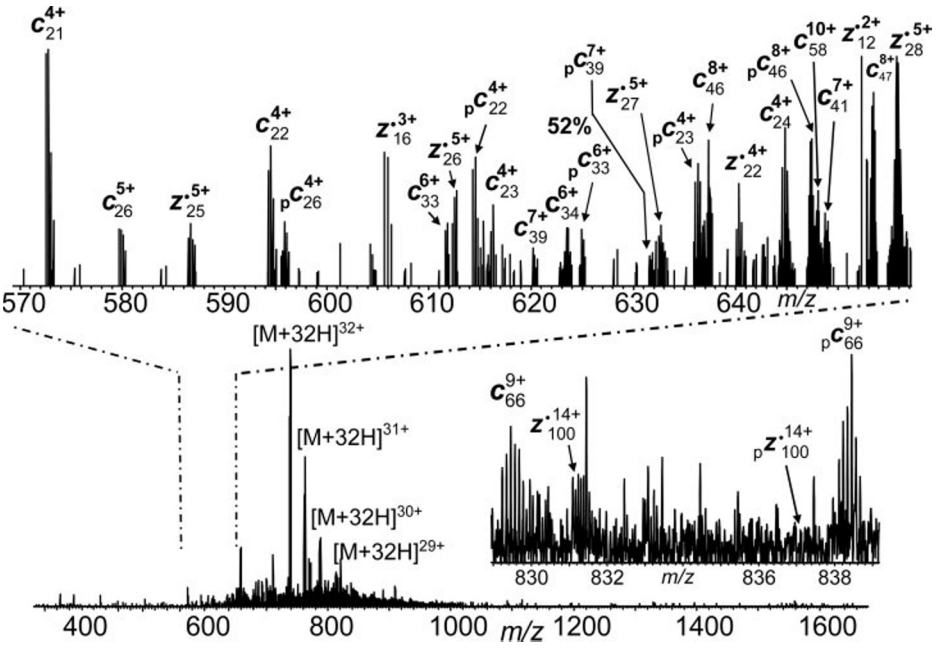

FIG. 2. **A representative ECD spectrum of monophosphorylated (*p*) human cTnI isoform III (M^{32+}) molecular ions at *m/z* 739.**

```
1   A D G Ⓢ Ⓢ D A A R E P R P A P A P I R R R Ⓢ Ⓢ N Ⓨ R A Ⓨ A Ⓣ
31  E P H A K K K Ⓢ K I Ⓢ A Ⓢ R K L Q L K Ⓣ L L L Q I A K Q E L
61  E R E A E E R R G E K G R A L Ⓢ Ⓣ R C Q P L E L A G L G F A
91  E L Q D L C R Q L H A R V D K V D E E R Ⓨ D I E A K V T K N
121 I Ⓣ E I A D L Ⓣ Q K I F D L R G K F K R P Ⓣ L R R V R I Ⓢ A
151 D A M M Q A L L G A R A K E Ⓢ L D L R A H L K Q V K K E D Ⓣ
181 E K E N R E V G D W R K N I D A L Ⓢ G M E G R K K K
```

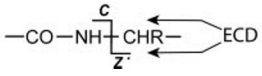

FIG. 3. **Product map from the ECD spectra for assignments to the DNA-predicted sequence of cTnI isoform III with the removal of three C-terminal residues, Phe-Glu-Ser.** Only reproducible fragments among the three replicates are shown. Ser (*S*), Thr (*T*), and Tyr (*Y*) residues are highlighted in *circles*.

idue was Ser^{22} from the qualitative data, we selected the six abundant *c* fragment ions between the N terminus and Ser^{22} as independent "internal standards" (as their relative abundances do not change between unphosphorylated and phosphorylated isoforms (supplemental Fig. 1)). The absolute abundances of the remaining unphosphorylated *c* ions from unphosphorylated and phosphorylated isoform III were normalized to these six fragments *intraspectrum*. The presence of multiple unphosphorylated *c* ions between the N terminus and Ser^{22} (six in our case) is advantageous as it allows for multiple independent measurements of the AR (Equation 1) for each fragment ion, greatly improving the precision of our quantification method. Moreover the abundances of all unphosphorylated *c* ions (normalized independently to the first six N-terminal *c* ions) were compared between the monophosphorylated and unphosphorylated isoform III. These abundance ratios revealed differences in fragment abundance caused by a phosphorylation event. To ensure statistical validity of our measurements, the experiments were repeated three times on the three most abundant charge states of both the unphosphorylated and monophosphorylated cTnI isoform III.

The abundance ratios of all unphosphorylated *c* ions from ECD of unphosphorylated and monophosphorylated isoform III are plotted against the amino acid sequence of cTnI (Fig. 5). A phosphorylation occupancy map of monophosphorylated cTnI is also illustrated in Fig. 5. The abundance ratios for the first six fragments (c_9, c_{15}, c_{18}, c_{19}, c_{20}, and c_{21}) from un- and monophosphorylated isoform III were approximately 1 (1.01 $\pm$ 0.1), indicating that their relative abundances did not change in the ECD spectra, which confirms that there is no phosphorylation site between the N terminus and Ser^{22}. The abundance ratio started to drop at c_{22} (Ser^{22}) and stayed at an average of 0.47 $\pm$ 0.05 between c_{23} and c_{69} indicating that 47% of Ser^{22} is unphosphorylated and 53% of the 23,634.728-*14* molecules are phosphorylated at Ser^{22}. The abundance ratios did not change appreciably between c_{23} and c_{69}, strongly suggesting that there are no phosphorylated residues between Ser^{23} and Glu^{69} including Ser$^{41/43}$ (Ser$^{41/43}$ in human cTnI; Ser$^{43/45}$ in mouse cTnI), and then decreased to 0.18 at c_{79} indicating that there is another major phosphorylation site between Gly^{69} and Cys^{79}. There are only two possible phosphorylation sites within this region, Ser^{76} and Thr^{77}, suggesting that the second dominant positional isomer was

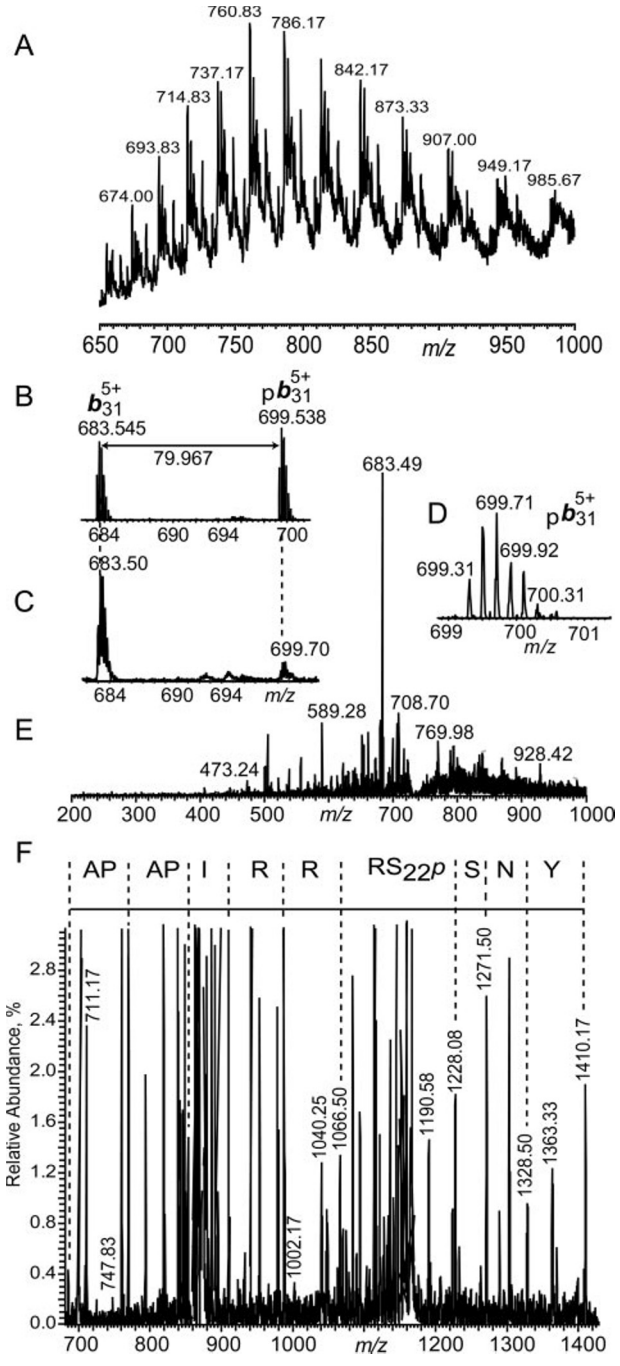

FIG. 4. **Confirmation of monophosphorylation site at Ser[22] by MS[3] ETD experiments.** *A*, low resolution ESI spectra of multiply charged intact cTnI molecular ions measured in the linear ion trap. *B*, partial high resolution IRMPD spectrum from the monophosphorylated cTnI isoform III 32+ molecular ion at *m/z* 740. *C*, partial linear trap CAD spectrum from the precursor molecular ion at *m/z* 740. *D*, a linear trap ultrazoom CAD scan showing the isotopically resolved monophosphorylated (*p*) b_{31}^{5+} fragment ion. *E*, linear trap CAD spectrum from the monophosphorylated cTnI isoform III 32+ molecular ion at *m/z* 740. *F*, ETD MS^3 spectrum of the monophosphorylated b_{31}^{5+} fragment ion. The region shows ETD doubly charged *c* fragment ions forming a sequence tag that is consistent with fully phosphorylated Ser[22] and unphosphorylated Ser[23].

phosphorylated at either of these two residues and accounted for 36% of phosphorylation occupancy of the 23,634.728-*14* molecules. As no *c* fragment ions were observed between these two residues, we cannot confidently assign the modification to either one. In addition, the abundance ratios remained at an average of 0.11 ± 0.08 between c_{79} and c_{113} suggesting the presence of a low level (10–12%) unidentified positional isomer(s) with likely phosphorylation site(s) between Glu[113] and the C terminus. Because no phosphorylated $z^{\bullet}$ fragment ions were found between the C terminus and $z^{\bullet}_{28}$ (S/N = 20), this minor basal phosphorylation site(s) is likely located between residues Glu[113] and Thr[180]; which contains five Thr, two Ser and no Tyr residues.

Confirmation of the Phosphorylation Site by Bottom Up Mass Spectrometry—To verify the presence of phosphorylation at Ser[76]/Thr[77], human cTnI was digested with Glu-C protease for 1 h, and the resulting peptides were separated by reverse phase HPLC and sequenced in a data-dependent manner using an LTQ Orbitrap. The resulting LC-MS/MS file was searched against a human data base using Mascot. A total of eight peptides matched the sequence of cTnI (International Protein Index entry 00244346) with a score of 45 and sequence coverage of 37% (supplemental Table 4). The peptide Lys-Gly-Arg-Ala-Lys-Ser-Thr-Arg-Cys-Gln-Pro-Leu-Glu-Leu-Ala-Gly-Leu-Gly-Phe-Ala-Glu was found to be monophosphorylated as confirmed by its accurate mass (calculated M_r = 2297.142-*1*; experimental M_r = 2297.147-*1*; 2.2 ppm; at *m/z* 766.389, 3+) as well as its linear trap MS^2 spectrum (Mascot score, 16) with a dominant neutral loss of 80 Da (Fig. 6 and supplemental Fig. 2 and Table 5). The structural fragments indicate that either Ser[6] or Thr[7] (Ser[76]/Thr[77] in the protein sequence) is esterified by a phosphoryl group, directly *qualitatively* confirming our interpretation of the high resolution and high accuracy top down ECD data. Considering that Glu-C digestion was performed on the mixture of many structurally similar isoforms of the same protein (over 30 intact molecular ions were observed in the full-scan FTICR spectrum) and the recovery of phosphopeptides after digestion is not quantitative, no conclusions on the phosphorylation occupancy of this site can be made from the bottom up experiments.

Localization of a Diphosphorylation Site at Ser[23] by Top Down MS^3 Mass Spectrometry—The diphosphorylated isoform III (M^{32+}) molecular ion was first isolated and dissociated by IRMPD in the ICR cell or by CAD in the LTQ. In each case a dominant diphosphorylated b_{31}^{5+} fragment (3572.620-*1*, 1.9 ppm) at *m/z* 715.91 was produced with two consecutive neutral losses of 80 Da because of the energetic nature of IRMPD and CAD (Fig. 7, *A* and *B*). It is also possible that a portion of the ions at *m/z* 683.545 and 699.538 can be un- and monophosphorylated b_{31}^{5+} fragments directly resulting from the diphosphorylated M^{32+} precursor ions. For the MS^3 experiments, the diphosphorylated M^{32+} molecular ions were first isolated and dissociated by CAD in a stand alone LTQ equipped with an ETD source. The resulting b_{31}^{5+} fragment

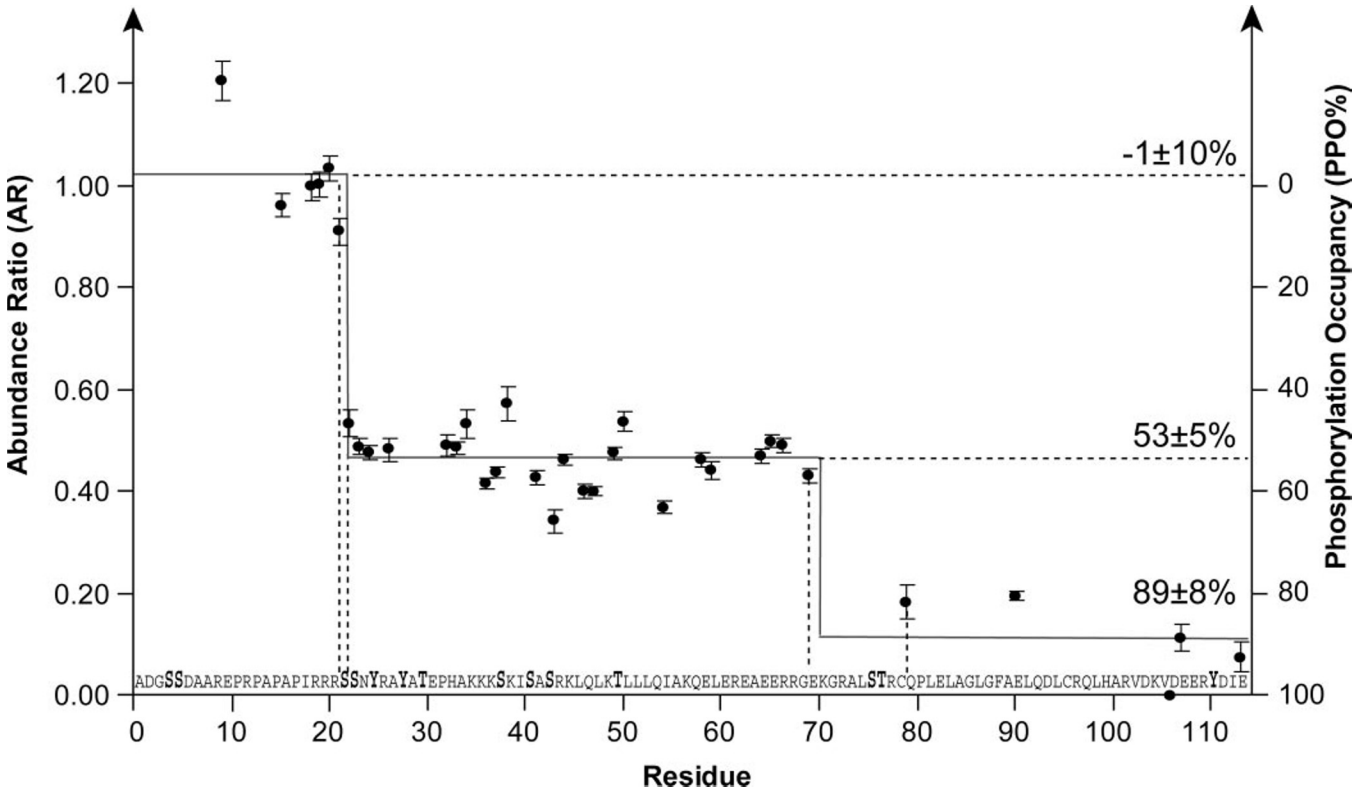

FIG. 5. **PPO% map of monophosphorylated cTnI isoform III.** The normalized absolute ARs of unphosphorylated *c* fragment ions from ECD spectra of both unphosphorylated (*m/z* 737) and monophosphorylated (*m/z* 740) molecular ions are plotted *versus* the amino acid sequence (only 114 N-terminal residues are shown). AR and PPO% were calculated according to Equations 1 and 2. The S. E. was calculated for each fragment AR ($n = 18$ (three replicates of six internal standard *c* ions)).

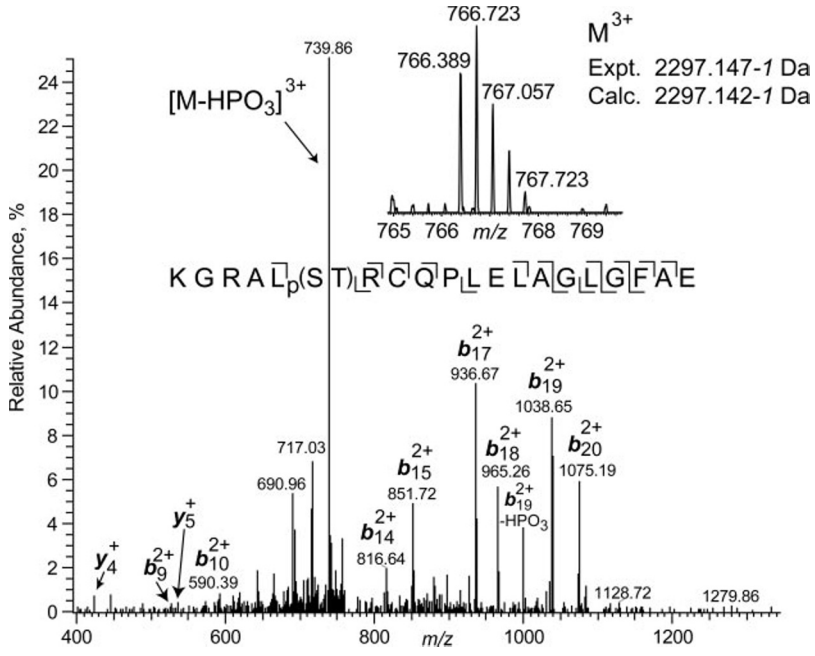

FIG. 6. **Conformation of phosphorylation site at Ser[76]/Thr[77] by bottom up mass spectrometry.** A CAD spectrum from the precursor ion (M^{3+}) at *m/z* 767 (*inset*), corresponding to a monophosphorylated (*p*) Glu-C peptide (sequence shown) from limited digestion of cTnI, is shown. *Calc.*, calculated; *Expt.*, experimental.

ions at *m/z* 715.88 were further isolated and fragmented using ETD where the corresponding doubly charged *c* ions were shifted by an additional 80 Da starting from the c_{23} fragment ion (Fig. 7*D*) compared with the *c* fragment ions in the ETD MS^3 spectrum obtained from the monophosphorylated isoform (Fig. 7*C* and supplemental Table 6). This indicated that

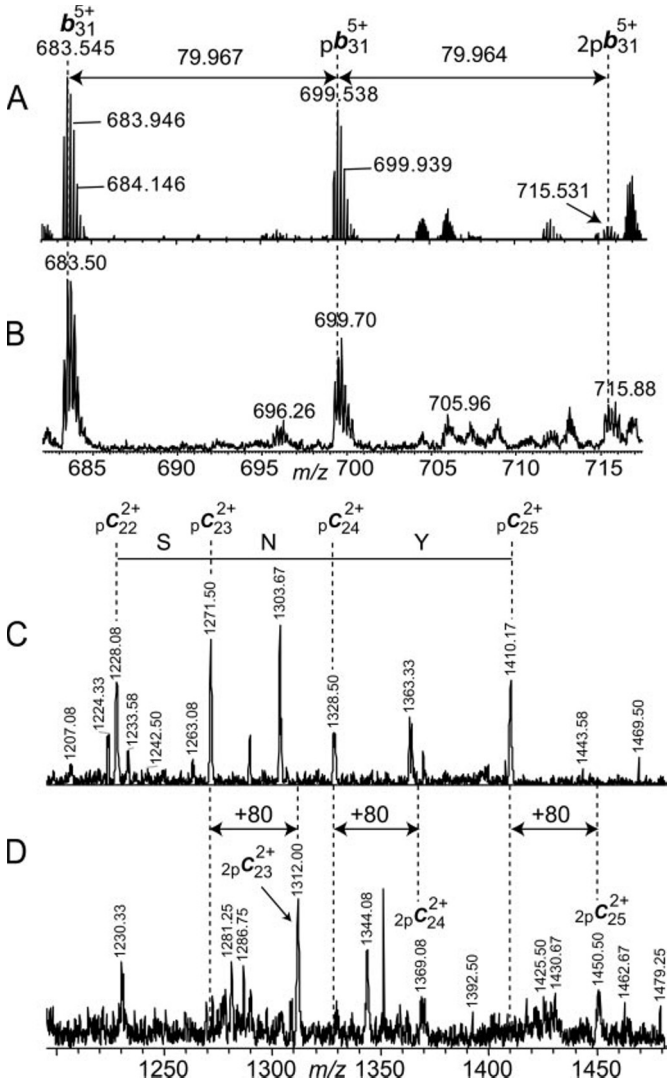

FIG. 7. **Localization of phosphorylated sites in diphosphorylated cTnI isoform III by MS³ ETD.** *A*, partial high resolution IRMPD spectrum of the precursor ion at *m/z* 742.092 corresponding to diphosphorylated isoform III (32+). *B*, partial low resolution CAD spectrum recorded in the linear trap on the same parent ion. *C*, partial ETD MS^3 spectrum of the monophosphorylated $b_{31}{}^{5+}$ fragment ion. The expanded region shows doubly charged *c* fragment ions forming a sequence tag that includes monophosphorylated (*p*) Ser^{22} and unphosphorylated Ser^{23}. *D*, partial ETD MS^3 spectrum of the diphosphorylated (*2p*) $b_{31}{}^{5+}$ fragment ion. The region shows ETD doubly charged *c* fragment ions forming a sequence tag that includes phosphorylated Ser^{22} and Ser^{23}.

among the diphosphorylated isomers of isoform III there was a significant portion of positional isomers with both Ser^{22} and Ser^{23} phosphorylated in the same molecule. Importantly occupancy of Ser^{23} was not detected in monophosphorylated species but was observed here in diphosphorylated cTnI ions. As no other abundant MS^2 fragments suitable for consecutive MS^3 analysis were observed in CAD or IRMPD spectra, further experiments to localize other possible phosphorylation sites in diphosphorylated isoform III were not undertaken.

DISCUSSION

Complex Molecular Heterogeneity of cTnI—The high resolution MS spectrum of cTnI reveals a substantial degree of heterogeneity where 36 distinct components of human cTnI were observed; albeit a parallel analysis of cTnI by SDS-PAGE showed only a single sharp band. A previous low resolution LC/MS and MALDI/MS analysis of human cTnI only reported up to eight heterogeneous cTnI components (55). The accurate molecular weights measured here by high resolution MS revealed a number of features of human cTnI. The removal of Met was confirmed in agreement with the amino acid sequence obtained from the Swiss-Prot database. In addition, all isoforms detected here were acetylated on the N-terminal Ala. Three different types of truncated products of cTnI were found resulting from truncations of C-terminal Glu-Ser, Phe-Glu-Ser, and Lys-Phe-Glu-Ser residues. This proteolytic C-terminal truncation of cTnI might correlate with altered cardiac function as the C terminus is highly conserved and may directly participate in the allosteric switch during Ca^{2+} activation of contraction (56). Mono- and diphosphorylations were observed in all four isoforms (I–IV) of cTnI. Oxidation was also observed that could possibly occur *in vivo* as a result of oxidative stress or *in vitro* from sample preparation or both. cTnI is known to be subject to extensive post-translational modification including phosphorylation, proteolysis, and oxidation under both physiological and pathological conditions (57). These modifications occurring either in the myocardium or after release into the general circulation could potentially provide insight into the history of cTnI present in the tissues and fluids of the body and ultimately be linked to disease etiology, pathogenesis, and prognosis.

Top Down MS with ECD for Quantification of Phosphorylated Positional Isomers—Top down ECD analysis of monophosphorylated cTnI isoform III suggested the existence of more than one positional isomer for monophosphorylated 23,634.728-*14* molecular ions. Because ECD is known to preserve labile post-translational modifications (37, 38, 42–45), the presence of a mixture of un- and monophosphorylated c_{22}–c_{113} fragment ions indicated the existence of at least one additional phosphorylation site located between Ser^{22} and the C terminus. Conversely if all phosphoryl groups were present only on Ser^{22} (the case of a single positional isomer), one would expect to see only phosphorylated c_{22}–c_{113} fragments.

To quantify the phosphorylated positional isomers, instead of directly measuring ratios of unphosphorylated to phosphorylated fragments in a single spectrum (analogous to what has been successfully done by Kelleher and co-workers (25) for a non-labile post-translational modification), we developed a new methodology by measuring the difference in relative abundance of the unphosphorylated *c* ions derived from ECD of unphosphorylated and monophosphorylated precursor ions. This is because ECD cleavage efficiency of the peptide

backbone bonds could be affected by the phosphate moiety in the neighborhood thereby altering the yield of the phosphorylated fragments (58) so that the relative abundances of phosphorylated *c* ions derived from ECD/ETD are *not* necessarily proportional to the size of the corresponding phosphorylated isomeric precursors. Hence a direct measurement of the abundance ratios of phosphorylated to unphosphorylated $c/z^{\bullet}$ ions within one spectrum would significantly compromise the accuracy in quantification of phosphorylated isomers.

In contrast, our method utilized only the unphosphorylated fragment ions first through *intraspectrum* normalization *versus* internal standard fragments followed by a comparison between ECD spectra of unphosphorylated and phosphorylated precursor ions, allowing for quantitative determination of partial phosphorylation occupancies of the corresponding sites as the abundance ratios revealed the difference attributed to phosphorylation events. Therefore, it is arguably a more accurate method for quantification of phosphorylation occupancies because of the physicochemical properties of phosphorylated polypeptides (25, 35, 53, 54).

Potential Physiological Implication of the New Phosphorylation Site—A new phosphorylation site was identified and quantified at residue Ser^{76}/Thr^{77} by top down ECD and confirmed by a Glu-C proteolytic digest. To our knowledge, this is the first experimental evidence for Ser^{76}/Thr^{77} as an *in vivo* phosphorylation site in human cTnI, although Ser^{76} is predicted to be a phosphosite based on an algorithm that detects kinase recognition motifs (PhosphoSite, Cell Signaling Technology). Moreover Kuo and co-workers (59) reported that Ser^{78} in bovine cTnI was slowly and incompletely phosphorylated by PKC *in vitro*. Interestingly human cTnI and bovine cTnI share 100% sequence identity for >20 residues flanking each side of this residue (Ser^{76} in human cTnI; Ser^{78} in bovine cTnI). Phosphorylation of cTnI by PKC occurs primarily on $Ser^{43/45}$ and Thr^{144}, resulting in alterations of calcium sensitivity and ATPase rate during contraction (3–7, 10). In the crystal structure of the human troponin complex obtained by Maeda and co-workers (60), Ser^{76}/Thr^{77} is exposed to solvent and likely to be accessible to kinases. In addition, it is possible that phosphorylation of Ser^{76}/Thr^{77} located at the end of an α-helix may serve to extend the helix by analogy with phosphorylation of $Ser^{41/43}$ to alter the rigidity of a lever arm in the heterotrimeric protein complex (4). Both the expression level of protein kinases and the phosphorylation state of myofilament proteins have been shown to be altered in end stage heart failure (9), but the status of Ser^{76}/Thr^{77} has not been investigated further in this context because of the lack of information on the storage and purification conditions for this commercially available human cTnI.

Ordered or Sequential Phosphorylation—Our top down MS/MS and MS^3 analysis of cTnI revealed Ser^{22} as a primary phosphorylation site in both mono- and diphosphorylated human cTnI, whereas Ser^{23} was only phosphorylated in the diphosphorylated species. Sequential (or ordered) phosphorylation of these serine residues on cTnI has been suggested based upon phosphorylation of synthetic peptides by PKA *in vitro* (61–64). In those studies, Ser^{23} was phosphorylated first followed by Ser^{22} at a ~10-fold slower rate. Differences in phosphorylation kinetics was also reported by Potter and co-workers (65) who treated mouse cTnI containing alanine substitutions with PKA *in vitro* and found that Ser^{23} was phosphorylated severalfold more rapidly than Ser^{22}. These authors suggested that Ser^{23} might be constitutively phosphorylated and that Ser^{22} phosphorylation may therefore be functionally more important. Here we found strong evidence for constitutive phosphorylation of Ser^{22} rather than for Ser^{23} in human cTnI. This apparent disagreement of our results with the literature may be explained by our analysis of the basal phosphorylation state of intact human cTnI phosphorylated *in vivo* in contrast to those previous *in vitro* studies (61–65). *In vivo*, Ser^{22} may be phosphorylated by kinases in addition to PKA, such as PKC (12, 66, 67), cyclic GMP-dependent protein kinase (10), and protein kinase D (14). Moreover one must consider the actions of phosphatases in the *in vivo* setting that may also dephosphorylate Ser^{23} faster than Ser^{22} such that Ser^{22} is the thermodynamically preferred site even though Ser^{23} is kinetically preferred. The need to study phosphosites that occur *in vivo* has been emphasized in recent studies because some of the *in vitro* sites appeared to be artifacts (68). In general, the basal phosphorylation state of cTnI has not been adequately established from any tissue source, so our characterization of these *in vivo* phosphorylation sites represents an important precedent for this protein. In fact, the basal state of post-translational modification is an important starting point in understanding regulation of any protein *in vitro* and *in vivo*.

Conclusion—Top down ECD and ETD mass spectrometry has been directly applied here for unraveling the molecular complexity of phosphorylated cTnI purified from human heart tissue. FTMS spectra of intact cTnI ions revealed a high degree of heterogeneity (over 30 different molecular ions) within a nominally pure sample of cTnI. Many of the ions were assigned to specific molecular species, and much of the heterogeneity was accounted for aided by the high mass accuracy and high resolution afforded by this technology. ECD and ETD dissociations of cTnI retained labile phosphoryl moieties and allowed for reliable localization of basally phosphorylated sites in human cTnI. Two major basal phosphorylation sites were characterized from monophosphorylated cTnI, one of which was an extensively studied PKA site, whereas the other was an almost completely unknown and uninvestigated site. Meanwhile a new methodology was also developed for quantification of the positional isomers with labile post-translational modifications. Top down MS^3 analysis of diphosphorylated cTnI revealed another PKA phosphorylation site and suggested sequential (or ordered) phosphorylation/dephosphorylation between these PKA sites. These new insights into cTnI structure and new capabilities afforded

by top down MS/MS will facilitate a deeper understanding of physiology and pathophysiology of this important human phosphoprotein. As shown here, top down MS/MS with ECD/ETD provides unique opportunities for 1) discovery of novel phosphorylation sites, 2) quantification of positional isomers even with labile phosphorylation, and 3) exploration of interdependencies between phosphorylation sites by different kinase/phosphatase systems.

Acknowledgments—We thank Dr. Fred McLafferty, Dr. Michael Senko, Dr. Joseph Loo, Dr. Stevan Horning, Raquel Solis, Lisa Xu, Tonya Second, Nate Evans, Matt Lawrence, and Ka Young Chung for helpful discussions.

* This work was supported by the Wisconsin Partnership Fund for a Healthy Future and the American Heart Association. The costs of publication of this article were defrayed in part by the payment of page charges. This article must therefore be hereby marked "*advertisement*" in accordance with 18 U.S.C. Section 1734 solely to indicate this fact.

[S] The on-line version of this article (available at http://www.mcponline.org) contains supplemental material.

¶ To whom correspondence may be addressed. Tel.: 608-263-9212; Fax: 608-265-5512; E-mail: yge@physiology.wisc.edu.

‖ To whom correspondence may be addressed. Tel.: 608-262-6941; Fax: 605-265-5512; E-mail: jwalker@physiology.wisc.edu.

REFERENCES

1. Solaro, R. J., and Rarick, H. M. (1998) Troponin and tropomyosin—proteins that switch on and tune in the activity of cardiac myofilaments. *Circ. Res.* **83,** 471–480
2. Kobayashi, T., and Solaro, R. J. (2005) Calcium, thin filaments, and the integrative biology of cardiac contractility. *Annu. Rev. Physiol.* **67,** 39–67
3. Huang, X. P., Pi, Y. Q., Lee, K. J., Henkel, A. S., Gregg, R. G., Powers, P. A., and Walker, J. W. (1999) Cardiac troponin I gene knockout—a mouse model of myocardial troponin I deficiency. *Circ. Res.* **84,** 1–8
4. Walker, J. W. (2006) Protein kinase C, troponin I and heart failure: overexpressed, hyperphosphorylated and underappreciated? *J. Mol. Cell. Cardiol.* **40,** 446–450
5. Pi, Y. Q., Kemnitz, K. R., Zhang, D. H., Kranias, E. G., and Walker, J. W. (2002) Phosphorylation of troponin I controls cardiac twitch dynamics—evidence from phosphorylation site mutants expressed on a troponin I-null background in mice. *Circ. Res.* **90,** 649–656
6. Pi, Y. Q., Zhang, D. H., Kemnitz, K. R., Wang, H., and Walker, J. W. (2003) Protein kinase C and A sites on troponin I regulate myofilament Ca^{2+} sensitivity and ATPase activity in the mouse myocardium. *J. Physiol. (Lond.)* **552,** 845–857
7. Wang, H., Grant, J. E., Doede, C. M., Sadayappan, S., Robbins, J., and Walker, J. W. (2006) PKC-bβII sensitizes cardiac myofilaments to Ca^{2+} by phosphorylating troponin I on threonine-144. *J. Mol. Cell. Cardiol.* **41,** 823–833
8. Babuin, L., and Jaffe, A. S. (2005) Troponin: the biomarker of choice for the detection of cardiac injury. *Can. Med. Assoc. J.* **173,** 1191–1202
9. van der Velden, J., Papp, Z., Zaremba, R., Boontje, N. M., de Jong, J. W., Owen, V. J., Burton, P. B. J., Goldmann, P., Jaquet, K., and Stienen, G. J. M. (2003) Increased Ca^{2+}-sensitivity of the contractile apparatus in end-stage human heart failure results from altered phosphorylation of contractile proteins. *Circ. Res.* **57,** 37–47
10. Layland, J., Solaro, R. J., and Shah, A. M. (2005) Regulation of cardiac contractile function by troponin I phosphorylation. *Cardiovasc. Res.* **66,** 12–21
11. Sakthivel, S., Finley, N. L., Rosevear, P. R., Lorenz, J. N., Gulick, J., Kim, S., VanBuren, P., Martin, L. A., and Robbins, J. (2005) In vivo and in vitro analysis of cardiac troponin I phosphorylation. *J. Biol. Chem.* **280,** 703–714
12. Noland, T. A., Jr., Guo, X. D., Raynor, R. L., Jideama, N. M., Averyhartfullard, V., Solaro, R. J., and Kuo, J. F. (1995) Cardiac troponin I mutants. Phosphorylation by protein kinases C and A and regulation of Ca^{2+}-stimulated MgATPase of reconstituted actomyosin S-1. *J. Biol. Chem.* **270,** 25445–25454
13. Buscemi, N., Foster, D. B., Neverova, I., and Van Eyk, J. E. (2002) p21-activated kinase increases the calcium sensitivity of rat Triton-skinned cardiac muscle fiber bundles via a mechanism potentially involving novel phosphorylation of troponin I. *Circ. Res.* **91,** 509–516
14. Haworth, R. S., Cuello, F., Herron, T. J., Franzen, G., Kentish, J. C., Gautel, M., and Avkiran, M. (2004) Protein kinase D is a novel mediator of cardiac troponin I phosphorylation and regulates myofilament function. *Circ. Res.* **95,** 1091–1099
15. Kelleher, N. L., Lin, H. Y., Valaskovic, G. A., Aaserud, D. J., Fridriksson, E. K., and McLafferty, F. W. (1999) Top down versus bottom up protein characterization by tandem high-resolution mass spectrometry. *J. Am. Chem. Soc.* **121,** 806–812
16. Kelleher, N. L. (2004) Top-down proteomics. *Anal. Chem.* **76,** 196A–203A
17. Ge, Y., Lawhorn, B. G., ElNaggar, M., Strauss, E., Park, J. H., Begley, T. P., and McLafferty, F. W. (2002) Top down characterization of larger proteins (45 kDa) by electron capture dissociation mass spectrometry. *J. Am. Chem. Soc.* **124,** 672–678
18. Ge, Y., ElNaggar, M., Sze, S. K., Bin Oh, H., Begley, T. P., McLafferty, F. W., Boshoff, H., and Barry, C. E. (2003) Top down characterization of secreted proteins from Mycobacterium tuberculosis by electron capture dissociation mass spectrometry. *J. Am. Soc. Mass Spectrom.* **14,** 253–261
19. Ge, Y., Lawhorn, B. G., Elnaggar, M., Sze, S. K., Begley, T. P., and McLafferty, F. W. (2003) Detection of four oxidation sites in viral prolyl-4-hydroxylase by top-down mass spectrometry. *Protein Sci.* **12,** 2320–2326
20. Sze, S. K., Ge, Y., Oh, H., and McLafferty, F. W. (2002) Top-down mass spectrometry of a 29-kDa protein for characterization of any posttranslational modification to within one residue. *Proc. Natl. Acad. Sci. U. S. A.* **99,** 1774–1779
21. Jebanathirajah, J. A., Pittman, J. L., Thomson, B. A., Budnik, B. A., Kaur, P., Rape, M., Kirschner, M., Costello, C. E., and O'Connor, P. B. (2005) Characterization of a new qQq-FTICR mass spectrometer for post-translational modification analysis and top-down tandem mass Spectrometry of whole proteins. *J. Am. Soc. Mass Spectrom.* **16,** 1985–1999
22. Zabrouskov, V., and Whitelegge, J. P. (2007) Increased coverage in the transmembrane domain with activated-ion electron capture dissociation for top-down Fourier-transform mass spectrometry of integral membrane proteins. *J. Proteome Res.* **6,** 2205–2210
23. Whitelegge, J., Halgand, F., Souda, P., and Zabrouskov, V. (2006) Top-down mass spectrometry of integral membrane proteins. *Expert Rev. Proteomics* **3,** 585–596
24. Xie, Y. M., Zhang, J., Yin, S., and Loo, J. A. (2006) Top-down ESI-ECD-FT-ICR mass spectrometry localizes noncovalent protein-ligand binding sites. *J. Am. Chem. Soc.* **128,** 14432–14433
25. Pesavento, J. J., Mizzen, C. A., and Kelleher, N. L. (2006) Quantitative analysis of modified proteins and their positional isomers by tandem mass spectrometry: human histone H4. *Anal. Chem.* **78,** 4271–4280
26. Zhai, H. L., Dorrestein, P. C., Chatterjee, A., Begley, T. P., and McLafferty, F. W. (2005) Simultaneous kinetic characterization of multiple protein forms by top down mass spectrometry. *J. Am. Soc. Mass Spectrom.* **16,** 1052–1059
27. Zabrouskov, V., Han, X. M., Welker, E., Zhai, H. L., Lin, C., van Wijk, K. J., Scheraga, H. A., and McLafferty, F. W. (2006) Stepwise deamidation of ribonuclease A at five sites determined by top down mass spectrometry. *Biochemistry* **45,** 987–992
28. Zabrouskov, V., Giacomelli, L., van Wijk, K. J., and McLafferty, F. W. (2003) New approach for plant proteomics. Characterization of chloroplast proteins of Arabidopsis thaliana by top-down mass spectrometry. *Mol. Cell. Proteomics* **2,** 1253–1260
29. Han, X. M., Jin, M., Breuker, K., and McLafferty, F. W. (2006) Extending top-down mass spectrometry to proteins with masses greater than 200 kilodaltons. *Science* **314,** 109–112
30. Meng, F. Y., Forbes, A. J., Miller, L. M., and Kelleher, N. L. (2005) Detection and localization of protein modifications by high resolution tandem mass spectrometry. *Mass Spectrom. Rev.* **24,** 126–134
31. Yates, J. R. (2000) Mass spectrometry—from genomics to proteomics. *Trends Genet.* **16,** 5–8

32. Gygi, S. P., and Aebersold, R. (2000) Mass spectrometry and proteomics. *Curr. Opin. Chem. Biol.* **4,** 489–494
33. Smith, R. D., Tang, K. Q., and Shen, Y. F. (2006) Ultra-sensitive and quantitative characterization of proteomes. *Mol. Biosyst.* **2,** 221–230
34. Chait, B. T. (2006) Mass spectrometry: bottom-up or top-down? *Science* **314,** 65–66
35. Kjeldsen, F., Savitski, M. M., Nielsen, M. L., Shi, L., and Zubarev, R. A. (2007) On studying protein phosphorylation patterns using bottom-up LC-MS/MS: the case of human α-casein. *Analyst* **132,** 768–776
36. McLafferty, F. W., Fridriksson, E. K., Horn, D. M., Lewis, M. A., and Zubarev, R. A. (1999) Biochemistry–biomolecule mass spectrometry. *Science* **284,** 1289–1290
37. Zubarev, R. A., Kelleher, N. L., and McLafferty, F. W. (1998) Electron capture dissociation of multiply charged protein cations. A nonergodic process. *J. Am. Chem. Soc.* **120,** 3265–3266
38. Zubarev, R. A., Horn, D. M., Fridriksson, E. K., Kelleher, N. L., Kruger, N. A., Lewis, M. A., Carpenter, B. K., and McLafferty, F. W. (2000) Electron capture dissociation for structural characterization of multiply charged protein cations. *Anal. Chem.* **72,** 563–573
39. Syka, J. E. P., Coon, J. J., Schroeder, M. J., Shabanowitz, J., and Hunt, D. F. (2004) Peptide and protein sequence analysis by electron transfer dissociation mass spectrometry. *Proc. Natl. Acad. Sci. U. S. A.* **101,** 9528–9533
40. Senko, M. W., Speir, J. P., and McLafferty, F. W. (1994) Collisional activation of large multiply charged ions using Fourier transform mass spectrometry. *Anal. Chem.* **66,** 2801–2808
41. Little, D. P., Speir, J. P., Senko, M. W., O'Connor, P. B., and McLafferty, F. W. (1994) Infrared multiphoton dissociation of large multiply-charged ions for biomolecule sequencing. *Anal. Chem.* **66,** 2809–2815
42. Shi, S. D. H., Hemling, M. E., Carr, S. A., Horn, D. M., Lindh, I., and McLafferty, F. W. (2001) Phosphopeptide/phosphoprotein mapping by electron capture dissociation mass spectrometry. *Anal. Chem.* **73,** 19–22
43. Kelleher, R. L., Zubarev, R. A., Bush, K., Furie, B., Furie, B. C., McLafferty, F. W., and Walsh, C. T. (1999) Localization of labile posttranslational modifications by electron capture dissociation: the case of γ-carboxyglutamic acid. *Anal. Chem.* **71,** 4250–4253
44. Hakansson, K., Cooper, H. J., Emmett, M. R., Costello, C. E., Marshall, A. G., and Nilsson, C. L. (2001) Electron capture dissociation and infrared multiphoton dissociation MS/MS of an N-glycosylated tryptic peptide to yield complementary sequence information. *Anal. Chem.* **73,** 4530–4536
45. Cooper, H. J., Hakansson, K., and Marshall, A. G. (2005) The role of electron capture dissociation in biomolecular analysis. *Mass Spectrom. Rev.* **24,** 201–222
46. Molina, H., Horn, D. M., Tang, N., Mathivanan, S., and Pandey, A. (2007) Global proteomic profiling of phosphopeptides using electron transfer dissociation tandem mass spectrometry. *Proc. Natl. Acad. Sci. U. S. A.* **104,** 2199–2204
47. Chi, A., Huttenhower, C., Geer, L. Y., Coon, J. J., Syka, J. E. P., Bai, D. L., Shabanowitz, J., Burke, D. J., Troyanskaya, O. G., and Hunt, D. F. (2007) Analysis of phosphorylation sites on proteins from Saccharomyces cerevisiae by electron transfer dissociation (ETD) mass spectrometry. *Proc. Natl. Acad. Sci. U. S. A.* **104,** 2193–2198
48. Ong, S. E., and Mann, M. (2005) Mass spectrometry-based proteomics turns quantitative. *Nat. Chem. Biol.* **1,** 252–262
49. Gygi, S. P., Rist, B., Gerber, S. A., Turecek, F., Gelb, M. H., and Aebersold, R. (1999) Quantitative analysis of complex protein mixtures using isotope-coded affinity tags. *Nat. Biotechnol.* **17,** 994–999
50. Ross, P. L., Huang, Y. L. N., Marchese, J. N., Williamson, B., Parker, K., Hattan, S., Khainovski, N., Pillai, S., Dey, S., Daniels, S., Purkayastha, S., Juhasz, P., Martin, S., Bartlet-Jones, M., He, F., Jacobson, A., and Pappin, D. J. (2004) Multiplexed protein quantitation in Saccharomyces cerevisiae using amine-reactive isobaric tagging reagents. *Mol. Cell. Proteomics* **3,** 1154–1169
51. Ong, S. E., Blagoev, B., Kratchmarova, I., Kristensen, D. B., Steen, H., Pandey, A., and Mann, M. (2002) Stable isotope labeling by amino acids in cell culture, SILAC, as a simple and accurate approach to expression proteomics. *Mol. Cell. Proteomics* **1,** 376–386
52. Mann, M. (2006) Functional and quantitative proteomics using SILAC. *Nat. Rev. Mol. Cell Biol.* **7,** 952–958
53. Steen, H., Jebanathirajah, J. A., Rush, J., Morrice, N., and Kirschner, M. W. (2006) Phosphorylation analysis by mass spectrometry. Myths, facts, and the consequences for qualitative and quantitative measurements. *Mol. Cell. Proteomics* **5,** 172–181
54. Carr, S. A., Huddleston, M. J., and Annan, R. S. (1996) Selective detection and sequencing of phosphopeptides at the femtomole level by mass spectrometry. *Anal. Biochem.* **239,** 180–192
55. Bunk, D. M., and Welch, M. J. (2006) Characterization of a new certified reference material for human cardiac troponin I. *Clin. Chem.* **52,** 212–219
56. Jin, J. P., Yang, F. W., Yu, Z. B., Ruse, C. I., Bond, M., and Chen, A. H. (2001) The highly conserved COOH terminus of troponin I forms a Ca^{2+}-modulated allosteric domain in the troponin complex. *Biochemistry* **40,** 2623–2631
57. Labugger, R., Simpson, J. A., Quick, M., Brown, H. A., Collier, C. E., Neverova, I., and Van Eyk, J. E. (2003) Strategy for analysis of cardiac troponins in biological samples with a combination of affinity chromatography and mass spectrometry. *Clin. Chem.* **49,** 873–879
58. Tsybin, Y. O., He, H., Emmett, M. R., Hendrickson, C. L., and Marshall, A. G. (2006) Toward automated de novo peptide sequencing and protein characterization by combined electron capture dissociation and activated-ion electron capture dissociation. *Mol. Cell. Proteomics* **5,** (suppl.) S269
59. Noland, T. A., Raynor, R. L., and Kuo, J. F. (1989) Identification of sites phosphorylated in bovine cardiac troponin I and troponin T by protein kinase C and comparative substrate activity of synthetic peptides containing the phosphorylation sites. *J. Biol. Chem.* **264,** 20778–20785
60. Takeda, S., Yamashita, A., Maeda, K., and Maeda, Y. (2003) Structure of the core domain of human cardiac troponin in the Ca^{2+}-saturated form. *Nature* **424,** 35–41
61. Keane, N. E., Quirk, P. G., Gao, Y., Patchell, V. B., Perry, S. V., and Levine, B. A. (1997) The ordered phosphorylation of cardiac troponin I by the cAMP-dependent protein kinase—structural consequences and functional implications. *Eur. J. Biochem.* **248,** 329–337
62. Perry, S. V., Patchell, V. B., Levine, B. A., and Quirk, P. G. (1996) Ordered phosphorylation of serine residues of peptides corresponding to the N-terminal domain of cardiac troponin I. *J. Muscle Res. Cell Motil.* **17,** 151–151
63. Quirk, P. G., Patchell, V. B., Gao, Y., Levine, B. A., and Perry, S. V. (1995) Sequential phosphorylation of adjacent serine residues on the N-terminal region of cardiac troponin-I—structure-activity implications of ordered phosphorylation. *FEBS Lett.* **370,** 175–178
64. Mittmann, K., Jaquet, K., and Heilmeyer, L. M. G. (1992) Ordered phosphorylation of a duplicated minimal recognition motif for cAMP-dependent protein-kinase present in cardiac troponin-I. *FEBS Lett.* **302,** 133–137
65. Zhang, R., Zhao, J. J., and Potter, J. D. (1995) Phosphorylation of both serine residues in cardiac troponin is required to decrease the Ca^{2+} affinity of cardiac troponin C. *J. Biol. Chem.* **270,** 30773–30780
66. Jideama, N. M., Noland, T. A., Raynor, R. L., Blobe, G. C., Fabbro, D., Kazanietz, M. G., Blumberg, P. M., Hannun, Y. A., and Kuo, J. F. (1996) Phosphorylation specificities of protein kinase C isozymes for bovine cardiac troponin I and troponin T and sites within these proteins and regulation of myofilament properties. *J. Biol. Chem.* **271,** 23277–23283
67. Kobayashi, T., Yang, X. F., Walker, L. A., Van Breemen, R. B., and Solaro, R. J. (2005) A non-equilibrium isoelectric focusing method to determine states of phosphorylation of cardiac troponin I: identification of Ser-23 and Ser-24 as significant sites of phosphorylation by protein kinase C. *J. Mol. Cell. Cardiol.* **38,** 213–218
68. Craft, G. E., Graham, M. E., Bache, N., Larsen, M., and Robinson, P. J. (2008) The in vivo phosphorylation sites in multiple isoforms of amphiphysin I from rat brain nerve terminals. *Mol. Cell. Proteomics* **7,** 1146–1161